

ORIGINAL ARTICLE



Structural response of hybrid timber - cold formed steel floors

Dan V. Bompa¹ | George Dance² | Alexandru Chira³ | Martin G. Walker¹ | Zsolt Nagy⁴

Correspondence

Dr. Dan V. Bompa
University of Surrey
School of Sustainability, Civil and
Environmental Engineering
GU2 7XH, Guildford, UK
Email: d.bompa@surrey.ac.uk

¹ School of Sustainability, Civil and
Environmental Engineering, Uni-
versity of Surrey, Guildford, UK

² Tony Gee and Partners, Ashford,
UK

³ ITEC, Haute école d'ingénierie et
d'architecture de Fribourg, HEIA-
FR, HES-SO University of Applied
Sciences and Arts Western Swit-
zerland

⁴ Technical University of Cluj-Na-
poca, Cluj-Napoca, Romania

Abstract

The paper examines the composite performance of hybrid steel-timber lightweight floor assemblies incorporating cold-formed steel (CFS) profiles and plywood (PW) flooring panels with varying degrees of shear connection achieved by means of self-drilling screws. Material, push-out, and three-point short-span floor tests with or without web openings were carried out. The results and observations from the tests provide a detailed insight into the inelastic properties and ultimate response of such floor systems. Push-out tests indicate that denser connector arrangements increase connection stiffness, while push-out and short beam tests suggest an optimum connector spacing equal to the beam depth for a balance between structural performance and constructability. The experimental observations indicate that the ultimate condition of the short composite beams was characterized by CFS web crippling under the load application point, followed by a pull-through of the self-drilling screws. Web openings reduced the strength of the floor elements compared to the members with full webs. Complementary numerical studies are undertaken using nonlinear finite element procedures which were validated against the beam tests, offering a detailed insight into the stress levels in the timber, steel, and connectors. Codified procedures for determining the capacity of composite CFS sections are compared with the test results, and guidance for the practical design and construction of such systems is given.

Keywords

Cold-formed steel, Timber floors, Composites, Material tests, Shear connections

1 Introduction

Combining cold-formed steel (CFS) members and timber sheet materials enable lightweight construction with structural, cost, and environmental benefits for low- and medium-rise construction [1]. CFS profiles with or without web holes are widely used in building floors to integrate services [2]. These systems have been used in floors, walls, and are suitable for monotonic and cyclic loading [3,4]. CFS C-sections can outperform most alternative construction materials due to their cost, strength-to-weight ratio, and ease of erection [5]. These sections are slender, thin-walled, and susceptible to different types of buckling, such as lateral-torsional, local, distortional, crippling, and bearing failure [6]. These failures are mostly due to the thin plate elements of C-section beams, which can be avoided or delayed by using stiffeners. Plywood (PW) boards, an engineered product made by stacking veneer layers and glued by resins, are commonly used as decking in light gauge steel systems. Combining CFS profiles and timber sheets with screws or bolts leads to superior structural performance due to developed composite action, exceeding the limitations of both materials used

separately. The performance of the system can be improved by increasing the degree of shear connection or applying stiffeners to the CFS sections [7].

Full-scale tests on chipboard-CFS C-section flooring demonstrated that reducing connector spacing had little influence on the structural performance but bonding with a class D4 polyurethane bonding adhesive increased flexural stiffness by 40% [8]. Similarly, bending and push-out experiments showed that the mechanical performance depends on the spacing of the connectors and the presence of adhesives [9]. Structural adhesives, while providing superior properties to dry connections, can increase the cost of the system and also limit disassembly and system separation at end-of-life. Numerous studies have investigated the performance of CFS composite systems for floors and walls in terms of flexural stiffness, moment capacity, and lateral torsional buckling restraint [8,9]. However, there is little information on the influence of timber sheeting and shear connections on other forms of buckling in CFS floor systems. This study examines the experimental response of CFS floor elements with varying degrees of shear connections through a set of pilot push-out and short-span three-point loading beam tests, including CFS sections

with and without web openings. Numerical simulations are used to validate the nonlinear procedures adopted in the paper, and the test results are compared with existing codes.

2 Experimental and numerical methods

This study included pilot shear connection tests and short-span beam tests with varying connection spacings, some with web openings, to assess the performance of lightweight floors incorporating CFS sections and PW boards. Push-out tests were carried out to investigate the influence of connector density, and beam tests were conducted to assess the effect of the floorboard on structural performance under concentrated load. The experimental results aimed at validating nonlinear procedures to enable further parametric studies on CFS-PW floor systems.

2.1 Materials

The specimens used S390 grade 254 mm deep and 54 mm wide CFS channel sections with lip stiffeners. Sections with a 1.5 mm plate thickness were chosen as they are commonly used in lightweight timber-steel floor systems. Web coupons were extracted for testing, measuring 200 mm in length and 25 mm in width at the centre, tapering to 50 mm at the ends. The tests were conducted using a 100kN Instron 1341 fatigue machine under displacement control following existing procedures [11]. Corrosion-resistant, self-drilling hex screws of 5.5 mm diameter and 38 mm length made of carbon steel were used as connectors.

A softwood PW material for interior application was selected for the flooring board. Based on an initial structural design assuming full composite action and limitations imposed by the testing arrangement, boards of 18 mm were considered. For the compression tests, $3 \times 260 \times 67 \times 54$ mm³ prismatic samples made of three 18 mm panels tied with water-resistant wood glue were manufactured. These were used to determine the stress-strain response, elastic modulus and compressive strength. To evaluate the uniaxial tension capacity, $3 \times$ dog-bone specimens with a length of 500 mm, an end cross-section of 100×18 mm and a middle section of 50×18 mm, were also tested. These tests were carried out in Instron machines at a displacement rate of 0.1 mm/min. The moisture content was $2.03 \pm 0.61\%$, obtained through existing guidance.

2.2 Steel-timber specimens

Push-out tests were carried out to evaluate the effect of different degrees of shear connection between steel and timber elements (Figure 1). Specimens consisting of two 550 mm long CFS C-sections were constructed with 18 mm thick 550×500 mm² PW sheets attached to both faces, with varying spacing and number of screws. The four specimens were named PO_x, where $x=1,2,3,5$ indicates the number of screw rows (Table 1). This corresponds with boards with a single row of screws, and screws spaced at 300, 200 and 100 mm, respectively. The specimens were tested to failure using a 1000 kN Instron machine at a displacement rate of 0.25 mm/min, with loading applied to the steel section through a PW spreader and ball seating. Transducers were used to measure displacement and record data for load-slip curves.

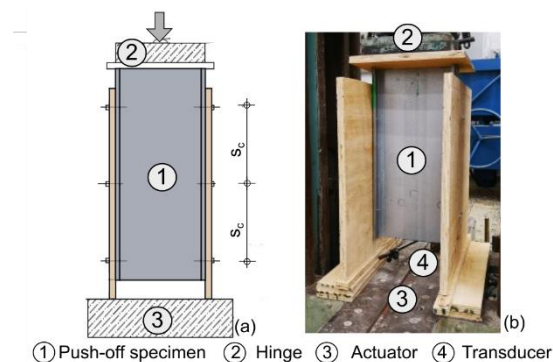


Figure 1 Push-out specimens a) schematic representation, b) testing

Four short-span beam tests were conducted to assess the composite action of lightweight floor systems incorporating CFS C-sections and PW boards using self-drilling screws (Figure 2). The beam specimens were named CPX_y, where X indicates the number of web openings and y indicates the shear connection density ($X=0,1,2$ for no, one or two openings on each side, respectively; $y=a,b$ for 300 and 200 mm spacing, respectively) (Table 1). The first 100 mm of beam ends were fitted with timber sections to avoid web buckling at the supports. Geometric imperfections of all specimens were measured before testing, which was in the range of 0.1t for the distortional and local modes, in which t is the plate thickness. The beams were positioned in a 600 kN Instron testing frame in three-point bending configuration and loaded gradually to failure at a rate of 0.25 mm/min using a displacement-controlled approach, typically used for testing composite/hybrid systems [13]. Transducers were used to record the deformations and the data was recorded by a logging unit.

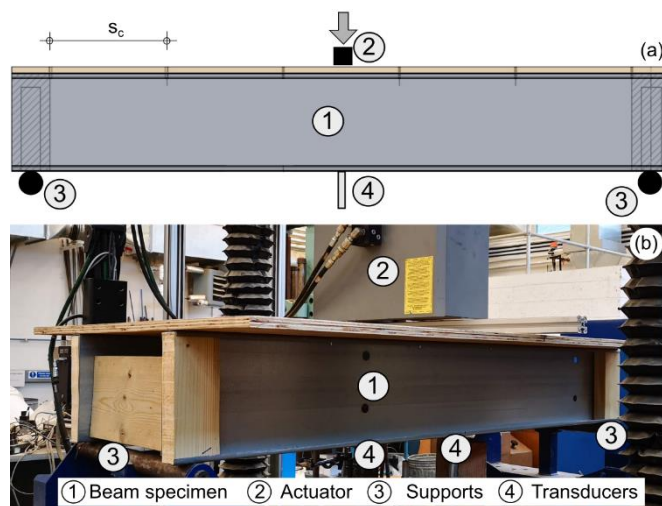


Figure 2 Beam specimens a) schematic representation, b) testing

2.3 Modelling procedures

The modelling procedures described below were adopted for the push-out and beam specimens, as well as for the PW boards in bending. The simulations on steel-timber members were employed to validate the considered procedures, obtain a detailed insight into the member kinematics and enable further parametric studies. The PW boards were modelled to validate the material properties through an inverse analysis, typically adopted for three or

four-point bending tests [13]. For the steel-timber members, the CFS profile was modelled using 4-node three-dimensional S4R shell elements with reduced integration and hourglass control, while C3D8R solid elements with reduced integration and hourglass control were used for modelling PW (Figure 3). R3D4 rigid three-dimensional elements were used to model the rollers for boundary conditions for the beam specimens. The steel profiles and PW were modelled using the PLASTIC material law using the measured material properties, available in ABAQUS [14]

Table 1 Specimen details

variant	Connector spacing s_c	Details
PO1	n/a single row	Push-out
PO2	300 mm	Push-out
PO3	200 mm	Push-out
PO5	100 mm	Push-out
CP0a	300 mm	Beam without openings
CP0b	200 mm	Beam without openings
CP1	200 mm	Beam with one opening
CP2	200 mm	Beam with two openings

Nonlinear FASTENERS with FAILURE were used to model the screws between the CFS profile and PW board, and a surface-to-surface contact (STANDARD) interaction with a friction coefficient of 0.30 between PW and CFS, and 0.40 between rollers and CFS was employed [14]. A buckling analysis was performed to consider the influence of local instabilities on buckling behaviour and capacity. An initial geometric imperfection with a scale of 0.1t was inserted based on the most representative case. A general static solver was used for the analysis step due to the high non-linearity caused by material properties, contact, and use of fasteners [15], and a 15 mm mesh was assigned to all elements after a mesh sensitivity study was performed. Only half of the composite beam geometry and of the push-out specimens were modelled using symmetry.

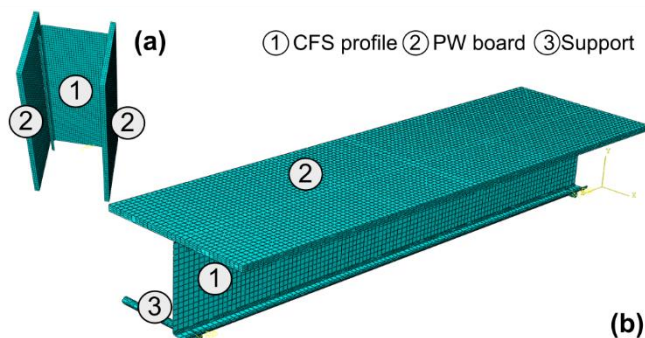


Figure 3 Numerical models for: a) push-out specimens, b) beams

3 Results and assessments

3.1 Material tests

The materials from the CFS sections, obtained through coupon tests had the following properties: yield strength $f_y=400\pm5.8$ MPa, ultimate strength $f_u=456\pm8.6$ MPa and a corresponding ultimate strain of $\epsilon_u=8.35\pm2.91\%$. As noted above, carbon steel self-drilling hex screws of 5.5 mm diameter \times 38 mm were used to connect the CFS flanges and PW boards. These were Grade 1022 with a minimum yield and ultimate strengths $f_{y,min}=360$ MPa and

$f_{u,min}=505$ MPa, respectively. The measured tensile and compressive strengths of the PW were $f_t=22.5\pm2.42$ MPa and $f_c=22.0\pm4.29$ MPa, respectively. The measured elastic stiffness was $E=3568$ MPa, which is about 10% less than the manufacturer elasticity perpendicular to the grain. Finally, the measured flexural strength of $f_r=28.4\pm3.59$ MPa.

3.2 Shear connection response

Various degrees of shear connection were tested in a push-out arrangement, including single-row screws, and with connector spacing of 100-, 200-, and 300-mm. Load slip curves of the four specimens and corresponding numerical simulations are presented in Figure 4. As a note, for improved reliability, average test curves from a minimum of three nominally identical tests would be needed. The connection stiffness was determined by calculating the gradient between 10% and 40% of the load-slip curves. Close inspection of the results indicates that stiffness remains constant for connection spacings below 200 mm (PO3) but decreases when spacing exceeds 200 mm. A 27% decrease between 200 mm (PO3) and 300 mm (PO2) spacing and a 56% decrease between 300 mm (PO2) and the single-row test sample (PO1), was observed. The optimal performance for ultimate load per connector was achieved at 200 mm spacing (PO3).

In terms of failure mode, specimens PO1, PO2, and PO3 (single-row, 300 mm, and 200 mm spacing, respectively) exhibited similar behaviour, with self-drilling screws rotating around the CFS flanges and some post-peak PW crushing. Increasing the number of connections can balance variations in PW material properties, leading to a more stable response. However, reducing connection spacing further may result in a grouping effect, reducing individual connection effectiveness. Specimen PO5 (100 mm spacing) failed due to local buckling of the steel profile and screw failure, indicating a stronger but unachieved capacity of the shear connection.

3.3 Beam response

Figure 5 plots the $P-\Delta$ curves of the tested beam specimens, in which the force P was recorded by the actuator and the Δ measured by a transducer at the underside of the PW board at the centre of the specimen, validated by machine displacement. Table 2 presents the peak force $P_{u,test}$ achieved by each member. The member stiffness K_{test} described below was evaluated between 10–40% of the peak load [16]. Specimen CP0a had a connector spacing of 300 mm and no web opening, while CP0b had a denser spacing of 200 mm. CP0b had slightly better performance with an elastic stiffness of $K_{test}=3597$ kN/m and ultimate capacity of $P_{u,test}=34.8$ kN, 5.30% and 5.46% higher, respectively, than CP0a. Increasing connector spacing slightly reduces structural performance. Both beams showed a fold in the top section of the CFS web under load, causing the top flange to pull away from the PW and leading to pull-through of the self-drilling screws. In CP0a, 6 screws failed due to pull-through, while CP0b had 8 screws fail.

Specimens with web openings had slightly lower elastic stiffness K_{test} and strength $P_{u,test}$ compared to CP0a. CP1 had one opening per side, with $K_{test}=3332$ kN/m and

$P_{u,test}=28.9$ kN, 7.4% and 12.2% lower than CP0a. CP2 had two openings per side, with $K_{test}=2932$ kN/m and $P_{u,test}=30.8$ kN, 18.5% and 6.4% lower than CP0a, showing a gradual reduction in stiffness with increasing openings. CP2 had higher strength than CP1 due to the opening location. As for CP0, 6-8 screws pulled through after buckling.

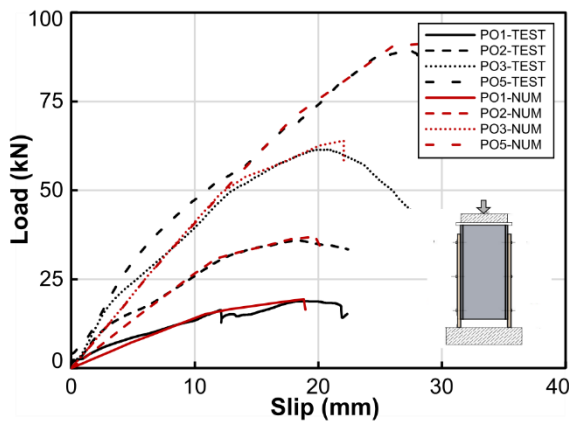


Figure 4 Comparative load-slip curves

All three-point loading test specimens failed due to web crippling of the CFS C-sections, which caused the top flange to lower. This type of failure occurs due to point loading at the supports or at the point of loading as evidenced in the literature [17]. Web crippling was followed by connector pull-out.

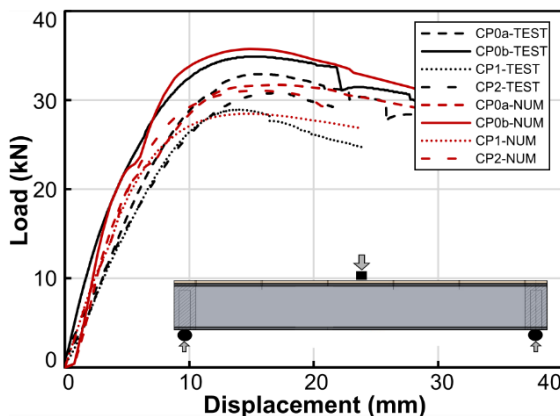


Figure 5 Comparative load-displacement curves

3.4 Numerical validation

As noted previously three-dimensional models were constructed to represent the push-out and beam specimens. Prior to undertaking the simulations of the composite members, PW in flexure was modelled to validate the wood material procedures. The numerical results indicate good agreement with the test curve indicating that the assumed PW material properties ($E=3$ GPa and $f_t=25$ MPa) are suitable for member modelling. Figure 4 illustrate in red curves the numerical prediction of the response of the push-out specimens PO1,2,3,5. As the load-slip curves indicate, the numerical model accurately predicted both the elastic response and peak point. A more sudden drop in capacity is observed in the numerical curve due to the inherent FASTNERS modelling adopted for the screws.

Table 2 summarizes the numerical results and Figure 5 shows the load-displacement ($P-\Delta$) curves. The force P was obtained from reference points in the models, and Δ was obtained at the mesh node corresponding to the location of the transducers used during the tests. The stiffness, yield strength, and overall deformations response were predicted with reasonable accuracy, as shown in Figure 5. Good agreement was obtained between the simulations and tests with a $P_{u,test}/P_{u,num} = 0.99$ and coefficient of variation COV of 0.02.

The analysis captures the experimental ultimate response, as seen in the close-up views of the specimen in the tests and the numerical von Mises strain maps (Figure 6). As observed from the strain maps, a concentration of stresses occurs under the load application points (marked with '3' in the figure), which produces local instability and buckling of the top flange. Further to an increase in load this instability is transferred to the web producing web crippling (marked with '4' in Figure 6). As shown above, the modelling procedures adopted in this study can closely capture the overall response of composite CPS-PW beams and can be further used for numerical sensitivity and parametric analyses of such systems.

Table 2 Numerical and test results

Specimen	P_{test} (kN)	P_{num} (kN)	P_{test}/P_{num} (-)
PO1	18.8	19.3	0.97
PO2	35.9	36.9	0.97
PO3	61.5	63.9	0.96
PO5	89.2	90.5	0.99
CP0a	32.9	31.7	1.04
CP0b	34.9	35.5	0.98
CP1	28.9	28.5	1.01
CP2	30.8	31.1	0.99

3.5 Code comparisons

To consolidate testing and numerical results, comparative assessments using code expressions on several aspects of the composite beam design were carried out. These included the elastic moment capacity of the beam, local buckling of the steel elements with and without composite action, crippling of the web, and distortional buckling of the CFS C-section using the guidance given in Eurocode 3 [19]. Close inspection of the code evaluations indicated that the elastic moment capacity was greater than the test capacity by above 140%.

To evaluate the local buckling of the steel section, the effective neutral axis and second moment area were calculated using only the tension and compression areas of the section. However, as the top flange was secured to the PW by self-tapping screws, the entire cross-sectional area of the top flange was virtually effective in compression, thus increasing the local buckling resistance. Both the local and distortional buckling resistance were by about 70% higher than the test value, confirming that these modes did not govern. Finally, the resistance of the web via crippling ($R_{w,R}$) was calculated using Equation (1), with values for $k_3=0.7+0.3(\Phi/90)^2$, $k_4=1.22-0.22(f_{yb}/228)$, and $k_5=\max(1.06-0.06r/t, 1)$ in which h_w is the web height, t is the web thickness, r the radius and f_{yb} is the yield strength.

It is worth noting that Equation (1) corresponds to the current version of Eurocode 3 [19], which has been updated. The expressions in the revised version of the code are likely to provide improved estimates.

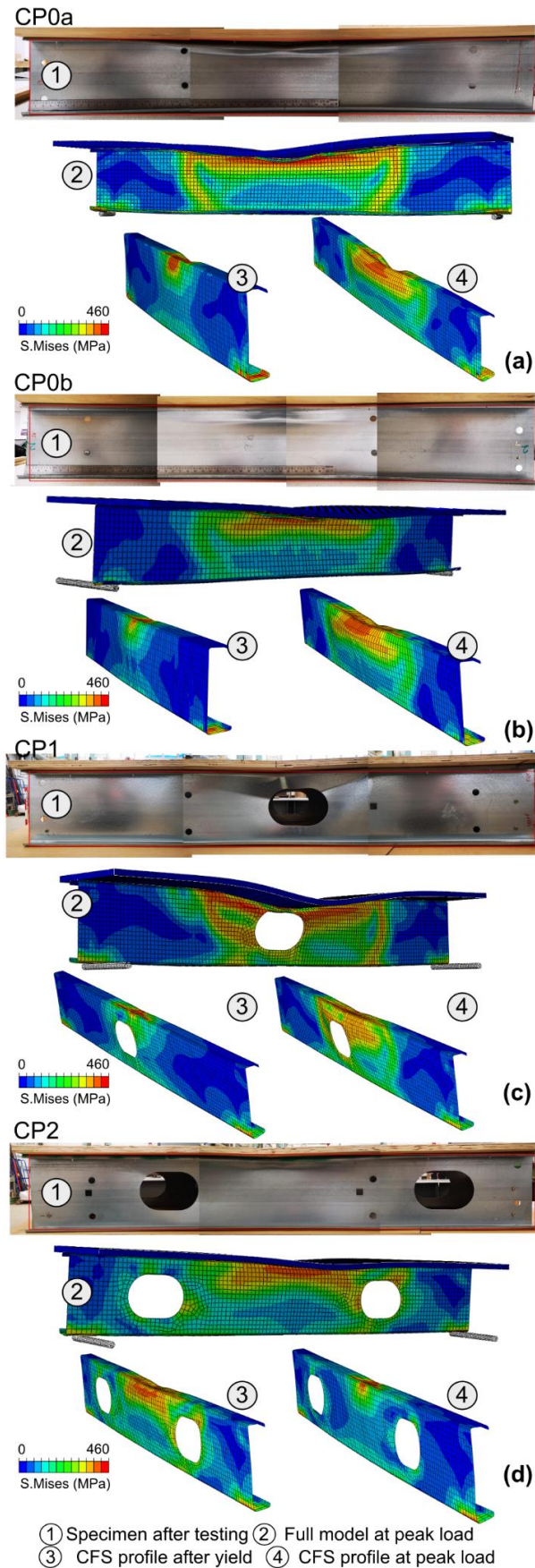


Figure 6 Stress distributions and failure representations

The width of the point load application s_s was taken as the width of the point load spreader plus the 45° spread caused by the PW underneath, represented as s_s . As discussed above in addition to web crippling, in tests pull-out of the screws from the PW occurred. Therefore, the pull-out resistance of the self-drilling screws was evaluated. The pull-out resistance of one self-drilling screw was calculated using Equation (2), in which d represented the nominal diameter of the fastener, t_{sup} was the thickness of the C-section flange and $f_{u,sup}$ was the ultimate tensile strength of the C-section.

$$R_{w,R} = k_3 k_4 k_5 \left[14.7 - \frac{h_w/t}{49.5} \right] \left[1 + 0.007 \frac{s_s}{t} \right] t^2 f_{yb} \quad (1)$$

$$F_{o,R} = 0.45 d t_{sup} f_{u,sup} \quad (2)$$

Figure 7 shows the strength evaluations described above, with crippling being the most likely form of failure. The composite beam failed at 42.3% higher loading than the assessed crippling failure of just the CFS C-sections, indicating composite action. To evaluate the contribution of the self-drilling screws, the number of the pulled-through connectors was multiplied by the resistance of a single connector. By accounting for the cumulative contribution of these two mechanisms improved estimates are obtained. It is suggested that, for composite CFS-PW systems such as those investigated in this paper, this approach can be adopted in design, although further experimental and numerical assessments are required.

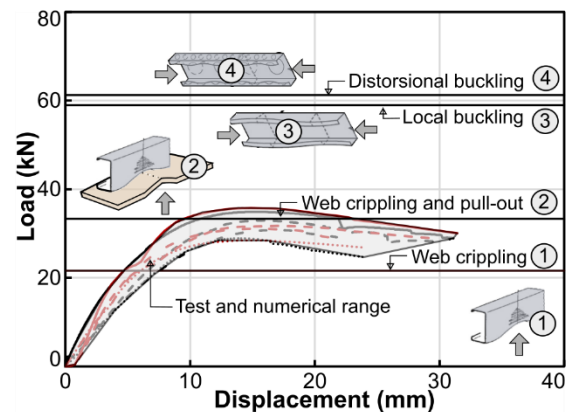


Figure 7 Code comparisons

4 Conclusions

The paper examined the composite performance of hybrid steel-timber light-weight floor assemblies incorporating cold-formed steel (CFS) profiles and plywood (PW) flooring panels, in which the degree of shear connection achieved by means of self-drilling screws was varied. A full account of material, push-out, and three-point short-span floor tests with or without web openings was carried out. Complementary numerical studies were undertaken using non-linear finite element procedures which were validated against the tests. The main remarks are outlined below.

The shear connection tests showed that stiffness remains constant for connection spacings below 200 mm but decreases by 27% from 200 mm and 300 mm, and by 56% from 300 mm to a single-row test sample. Increasing the connector spacing from 200 mm to 300 mm slightly re-

duces the performance of composite beam members without web openings. Specimens with web openings had slightly lower strength compared to the beams without openings. All beams failed through CFS web crippling and pull-through of the self-drilling screws. Based on these tests it is shown that the optimal performance considering mechanical properties and constructability is achieved at 200 - 300 mm spacing.

The modelling procedures adopted in this study, which include three-dimensional shell elements for CFS, solid elements with reduced integration and hourglass control for the PW, and combined nonlinear fasteners with failure for shear connectors and a surface-to-surface contact interaction between CFS-PW, were able to closely capture the overall response of composite CPS-PW beams. These procedures can be employed for numerical sensitivity and parametric analyses to improve the expressions for quantifying the influence of composite action on the web crippling resistance of such systems.

Acknowledgements

The authors acknowledge the support provided by the University of Surrey for materials and experimental facilities. The numerical research was carried out under the project "Modélisation non linéaire des éléments structurels et des assemblages dans la construction en bois (NoLiMoBois) (115048) a grant of the HES-SO University of Applied Sciences and Arts Western Switzerland.

References

- [1] Zhang, S. and Xu, L., 2022, April. Vibration serviceability evaluation of lightweight cold-formed steel floor systems. *Structures*, 38, pp. 1368-1379.
- [2] Chen, B., Roy, K., Fang, Z., Uzzaman, A., Chi, Y. and Lim, J.B., 2021. Web crippling capacity of fastened cold-formed steel channels with edge-stiffened web holes, un-stiffened web holes and plain webs under two-flange loading. *Thin-Walled Structures*, 163, p.107666.
- [3] Gatheeshgar, P., Poologanathan, K., Thamboo, J., Roy, K., Rossi, B., Molkens, T., Perera, D. and Navaratnam, S., 2021, April. On the fire behaviour of modular floors designed with optimised cold-formed steel joists. In *Structures* (Vol. 30, pp. 1071-1085).
- [4] Lawson, R.M., Kermani, A., Stergiopoulos, M., Coste, G. and Way, A., 2020. Diaphragm action in light steel framing by sheathing boards. *Engineering Structures*, 220, p.110952.
- [5] Dubina, D., Fülöp, L., Ungureanu, V., Szabo, I. and Nagy, Z., 2000, October. Cold-formed steel structures for residential and non-residential buildings. In *Proceedings of the 9th International Conference on Metal Structures*, Timisoara, Romania (pp. 19-22).
- [6] Trahair, N.S., Bradford, M.A., Nethercot, D.A. and Gardner, L., 2017. The behaviour and design of steel structures to EC3. CRC Press.
- [7] Sahin, B., Bravo-Haro, M.A. and Elghazouli, A.Y., 2022. Assessment of cyclic degradation effects in composite steel-concrete members. *Journal of Constructional Steel Research*, 192, p.107231.
- [8] Raffoul, S., Moutaftsis, D., Heywood, M. and Rowell, M., 2019. Composite behaviour of cold-formed steel-timber floors. *ce/papers*, 3(5-6), pp.372-380.
- [9] Kyvelou, P., Gardner, L. and Nethercot, D.A., 2017. Testing and analysis of composite cold-formed steel and wood-based flooring systems. *Journal of Structural Engineering*, 143(11), p.04017146.
- [10] Selvaraj, S. and Madhavan, M., 2020. Structural behaviour and design of plywood sheathed cold-formed steel wall systems subjected to out of plane loading. *Journal of Constructional Steel Research*, 166, p.105888.
- [11] Mujdeci, A., Bompa, D.V. and Elghazouli, A.Y., 2021. Confinement effects for rubberised concrete in tubular steel cross-sections under combined loading. *Archives of Civil and Mechanical Engineering*, 21, pp.1-20.
- [12] Mujdeci, A., Guo, Y.T., Bompa, D.V. and Elghazouli, A.Y., 2022. Axial and bending behaviour of steel tubes infilled with rubberised concrete. *Thin-Walled Structures*, 181, p.110125.
- [13] Tjibea, C. and Bompa, D.V., 2020. Ultimate shear response of ultra-high-performance steel fibre-reinforced concrete elements. *Archives of Civil and Mechanical Engineering*, 20, pp.1-16.
- [14] DSS (Dassault Systèmes Simulia Corp). 2018. ABAQUS, Analysis user's manual Johnston, RI, USA
- [15] Moharram, M.I., Bompa, D.V., Xu, B. and Elghazouli, A.Y., 2022. Behaviour and design of hybrid RC beam-to-steel column connections. *Engineering Structures*, 250, p.113502.
- [16] Vlach, T., Chira, A., Laiblová, L., Fiala, C., Novotná, M. and Hájek, P., 2015. Numerical Simulation of Cohesion Influence of Textile Reinforcement on bending performance of plates prepared from High Performance Concrete (HPC). In *Advanced Materials Research* (Vol. 1106, pp. 69-72). Trans Tech Publications Ltd.Hass, R.
- [17] ECCS (European Convention for Constructional Steelwork) 1986. Recommended testing procedure for assessing the behaviour of structural steel elements under cyclic loads. ECCS.
- [18] Beshara, B., Schuster, R. M., 2000. Web Crippling of Cold Formed Steel C-and Z- Sections. CCFSS Proceedings
- [19] CEN (European Committee for Standardization), 2005. EN 1993 Eurocode 3: design of steel structures. Brussels